Water Wave Instability Induced by a Drift Layer

by

E. A.Caponi

H. C. Yuen

F. A. Milinazzo

P. G. Saffman

November 1989

Water wave instability induced by a drift layer

E.A. Caponi and H.C. Yuen
TRW Redondo Beach, CA 90278

F.A. Milinazzo
Royal Roads Military College, Victoria, B.C.

P.G. Saffman
Caltech, Pasadena, CA 91125

A simple instability mechanism by which water waves can extract energy from a shear flow is isolated. A cubic equation is derived which provides the instability criteria and the growth rate. This mechanism is effective only if the surface drift velocity exceeds the minimum wave speed, which is approximately 23 cm/s in water, and only if the drift layer thickness exceeds a minimum value which is comparable with the unstable wavelength. In the situation of a sufficiently strong wind blowing over a flat calm, this mechanism is triggered early in the development stage, and appears to dominate the initial growth stages of centimeter waves.

1. Introduction

In recent work, Milinazzo & Saffman (1989) have studied the effect of a thin drift layer on the properties of finite amplitude capillary-gravity waves of permanent form on deep water. It was noticed that for certain values of the parameters, i.e. wavelength, surface tension, gravity, there were no real solutions for waves of small amplitude. The existence of complex wave speeds means that the waves are unstable, and in particular if the wave speed is complex for very small wave heights, it means that the plane interface is unstable to disturbances with wavelengths in the range for which steady solutions do not exist.

In the present paper, we investigate this instability directly by considering the case of infinitesimal waves of wavelength λ on a drift layer of thickness Δ containing vorticity $-\Omega$. It is convenient to formulate the problem as one of steady motion in which the wave speed c is real. Imaginary roots of the equation for c correspond to unstable disturbances growing like $z^{k c_i t}$, where $k = 2\pi/\lambda$ and $c_i = \mathrm{Im}\, c$.

We then follow closely the notation of Milinazzo & Saffman. The shape of the upper interface $H_1(x)$, the stream function $\Psi_1(x,y)$ in the drift layer, the shape of the lower interface between the drift layer and the irrotational flow $H_2(x)$, and the stream function in the irrotational fluid $\Psi_2(x,y)$ are

$$
\left.
\begin{aligned}
H_1 &= e_1 \cos kx, \\
\Psi_1 &= \tfrac{1}{2}\Omega y^2 + \left(a_1 e^{ky} + b_1 e^{-ky}\right)\cos kx, \\
H_2 &= -\Delta + e_1 \cos kx, \\
\Psi_2 &= -cy + d_1 e^{ky}\cos kx + \text{const.}
\end{aligned}
\right\}
\qquad (1.1)
$$

The boundary conditions, that the interfaces are streamlines and that the pressure is continuous across them, are linearised and applied on $y = 0$ and $y = -\Delta$. The calculation is straightforward and details of the manipulations are omitted. After some algebra we

2

obtain a cubic equation for $\theta = (c - \Omega\Delta)/c_o$,

$$\theta^3 + \theta^2\left(q + \tfrac{1}{2}\beta(1 - e^{-2q/\beta})\right) + \theta\left(-1 + \beta q - \tfrac{1}{2}\beta^2(1 - e^{-2q/\beta})\right) - q + \tfrac{1}{2}\beta(1 - e^{-2q/\beta}) = 0,$$

(1.2)

where

$$q = \frac{\Omega\Delta}{c_o}, \quad \beta = \frac{\Omega}{2\pi f_o}, \quad c_o = \sqrt{\frac{g\lambda}{2\pi} + \frac{2\pi T}{\lambda}}, \quad f_o = \frac{c_o}{\lambda}.$$

(1.3)

The wave speed $c = (\theta + q)c_o$. Note that if $q = 0$, we obtain $c/c_o = \pm 1$ and $c = 0$. If $\beta = 0$, $q > 0$, then $c/c_o = q \pm 1$ and $c = 0$. Also, $q \rightarrow -q$ corresponds to $\theta \rightarrow -\theta$.

The curious and unexpected feature of the equation for c is that there is a range of values of q and β for which c is imaginary. This means that given Ω and Δ, the plane interface is spontaneously unstable to disturbances of wavelength λ such that the values of q and β fall in the unstable region shown in figure 1. This region is calculated as follows

Take

$$\left.\begin{aligned}
a &= 1, \\
b &= \tfrac{1}{3}\left(q + \tfrac{1}{2}\beta(1 - e^{-2q/\beta})\right), \\
\tilde{c} &= \tfrac{1}{3}\left(-1 + \beta q - \tfrac{1}{2}\beta^2(1 - e^{-2q/\beta})\right), \\
d &= -q + \tfrac{1}{2}\beta(1 - e^{-2q/\beta}),
\end{aligned}\right\}$$

(1.4)

$$H = a\tilde{c} - b^2, \quad G = a^2 d - 3ab\tilde{c} + 2b^3.$$

(1.5)

Then

$$D = D(q, \beta) = (G^2 + 4H^3)/a^2$$

(1.6)

is the discriminant of the cubic. The roots are real if $D < 0$. If $D > 0$, there are two imaginary roots. When $D = 0$, the equation has two equal roots $-\sqrt{-H}\,\mathrm{sgn}\,G$. Instability occurs for those values of λ for which

$$D\left(\frac{\Omega\Delta}{c_o(\lambda)}, \frac{\Omega\lambda}{2\pi c_o(\lambda)}\right) > 0.$$

(1.7)

The instability boundary in figure 1 is the locus $D(q, \beta) = 0$. The wedge of instability has asymptotes $q \sim (3\beta)^{1/3}$ and $q \sim 1.83\beta$. The wedge is exponentially thin near its tip, where it asymptotes the line $\beta = q - 1$.

3

The dimensional growth rate of the instability is

$$\sigma = 2\pi f_o \theta_i = \sqrt{3}\,\pi f_o |Q + H/Q|, \tag{1.8}$$

where $\theta_i = \operatorname{Im}\theta$, $\theta_r = \operatorname{Re}\theta$, and

$$Q^3 = \tfrac{1}{2}(-G + \sqrt{G^2 + 4H^3}). \tag{1.9}$$

The phase speed is

$$c_P = u + c_o\theta_r = u - bc_o - \tfrac{1}{2}c_o(Q - H/Q). \tag{1.10}$$

The transition from real to imaginary wave speeds is associated with the coalescence of two of the real speeds. It is found that it is the two smaller speeds which coincide, so the unstable waves will propagate somewhat slower than the propagating wave mode which has phase speed $u - bc_o + c_o(Q - H/Q)$.

A situation close to that examined here has been studied by Voronovich, Lobanov & Rybak (1980), the difference being that they have a vortex sheet at the lower boundary of the wind drift layer. They identify a bubble of instability associated with the coalescence of eigenvalues when the vortex sheet is weak (compare MacKay & Saffman 1986), but for reasons that are not understood the instability seems to disappear when the vortex sheet strength vanishes.

2. Results

The wedge in figure 1 shows that there is no instability unless $q > 1$, i.e. $u \equiv \Omega\Delta > c_m$, where $c_m = (4gT)^{1/4}$ is the minimum phase speed and occurs when $\lambda = \lambda_m = 2\pi\sqrt{T/g}$. Thus this mechanism will not produce waves until u exceeds a critical value. Note that this criterion is independent of the air density and air motion.

Suppose now that u is fixed greater than c_m. When, for example, the drift layer is caused by wind, a typical value of u is 30 cm/sec (4% of mean wind speed U of 15 knots at a height of 10m). For $g = 981$ cm/sec^2 and $T = 72$ dynes/cm, $c_m = 23$ cm/sec and $\lambda_m = 1.7$ cm. For each value of λ, such that

$$u > c_o(\lambda) > c_m, \tag{2.1}$$

the value of $q = u/c_o$ is greater than 1, and hence there is instability if Δ is such that $\beta = u\lambda/(2\pi c_o\Delta)$ lies in the unstable range shown in figure 1. The range of λ given by (2.1) is

$$\lambda_{\max} = \lambda_m \left[(u/c_m)^2 + \sqrt{(u/c_m)^4 - 1}\right] > \lambda > \lambda_m \left[(u/c_m)^2 - \sqrt{(u/c_m)^4 - 1}\right] = \lambda_{\min}. \tag{2.2}$$

It is more convenient for the interpretation of the results to suppose that u/c_m is given and examine the range of λ in which unstable waves exist for a range of values of Δ/λ_m. In figure 2, we show plots of the range of λ/λ_m vs Δ/λ_m for which there is instability. It can be seen that there is no instability unless Δ exceeds a minimum Δ_{crit}. Also shown is the point of maximum dimensionless growth rate $\sigma_{\max}/f_m$, where $f_m = c_m/\lambda_m$ is the frequency of the minimum speed capillary gravity wave , and the contour where the growth rate is one-half of the maximum.

The dependence of $\lambda_{\text{crit}}/\lambda_m$, λ^+/λ_m, $\lambda_{\max}/\lambda_m$, and $\lambda_{\min}/\lambda_m$ is shown in figure 3(a). The superfix $^+$ denotes values at the point of maximum growth rate, crit refers to values at the nose where $\Delta = \Delta_{\text{crit}}$. Figure 3(b) shows the variation of Δ^+/λ_m and $\Delta_{\text{crit}}/\lambda_m$. Figure 3(c) shows the phase speeds and the growth rates. It can be shown that as $u/c_m \rightarrow 1$,

$\lambda_{\text{crit}}/\lambda_m \sim 1 - 2(u/c_m - 1)$, $\Delta_{\text{crit}}/\lambda_m \sim 1/2\pi(u/c_m - 1)^{-1}$ and σ_{max}/f_m is exponentially small. The phase speed of the unstable modes approaches zero as $u/c_m \to 1$, and the phase speed of the stable mode at the critical point aproaches $2c_m$. This is consistent with the idea that the drift layer convects the waves with a velocity u, and the instability can be thought of as a choking of the modes propagating against the drift layer.

3. Application to the generation of waves by wind

These results apply to the generation of waves by wind where the wind-induced surface drift velocity u is greater than the minimum wave speed of 23 cm/s. Note that even after the wind speed criterion is met, the instability requires the drift layer to exceed a minimum thickness, the value of which is dependent on wind speed and decreases with increasing wind speed. For a given wave length, there is also a maximum drift layer thickness beyond which the mechanism disappears, so that the amplification of each wavelength is confined to a specific growth stage.

Another interesting characteristic of this mechanism is that it is indirect: the wave extracts energy from the wind drift layer which in turn receives energy from the wind. This is in contrast with other wind-wave generation mechanisms such as that proposed by Phillips (1957) and Miles (1957).

Adopting the empirical relationship that $u = 0.04U$, where U is the wind speed measured at 10 m above water, the critical wind speed for the present instability mechanism to take effect would be $U \doteq 6$ m/s. A model can be constructed for the development of waves under wind due to this mechanism which can be compared with laboratory experiment. Consider the situation where the water surface is initially flat and at $t = 0$ the wind is turned on. At wind speeds greater than 6 m/s, the drift layer is expected to be turbulent and grow like $\Delta = \kappa u_* t$, where u_* is the friction velocity in the air typically having a value of about 4% of the wind speed at 10 m and κ is an empirical constant taken by Baum (1977) to be $\kappa = 0.25\sqrt{\rho_a/\rho} = 8.3\,10^{-3}$, where ρ_a is the air density. When the drift layer thickness exceeds the minimum thickness, the surface will become unstable to this mechanism. As the wind drift layer continues to thicken, a broader spectrum of waves become unstable, and the most unstable wavelength lengthens, see figure 2. Further thickening of the wind drift layer will result in the instability separating into two regimes, one for waves longer than the wave with minimum wave speed (gravity branch) and the other for waves shorter (capillary branch), with the growth in the gravity branch dominating. However, since the growth rate decreases as the wind drift layer thickens beyond Δ^+ (see figure 2),

7

this mechanism is expected to eventually give way to other processes of wave growth, such as the Miles mechanism or nonlinear wave-wave interactions.

As an example, we take $U = 10$ m/s, so that $u_* = u = 40$ cm/s and $u/cm = 1 \cdot 73$. From figure (3b), the minimum drift layer thickness is approximately 3.4 mm. This would take less than 1 second to establish. The development of an initial spectrum due to this instability mechanism is modelled by the equation

$$\frac{da(\lambda, t)}{dt} = \sigma(\lambda, t)\, a(\lambda, t), \tag{3.1}$$

where $a(\lambda, t)$ is the amplitude of the Fourier coefficient of the spectrum of wavelength λ. Note that with u, λ and $\Delta = \Delta(t)$ given, $\sigma(\lambda, t)$ is determined from equation (1.8).

Figure 4 shows the wavenumber spectrum at various stages of development from background noise (10–8) for $u/c_m = 2$ from $t = 0$ sec to $t = 4$ sec. The instability first appears at about 0.8 sec. By $t = 2$ sec, the spectral peak has grown by nearly 8 decades, and has downshifted from $k = 700$/m (near λ_{crit}) to $k = 380$/m (near λ_m). Subsequent development becomes one of gradual spreading of the spectrum towards lower wavenumbers, but the spectral peak remains unchanged at about the wavenumber corresponding to the wavelength of minimum wavespeed. The rate of spectral development is a sensitive function of u as well as of the rate of thickening of the drift layer, both of which have to be related to wind speed empirically. This is another reminder that the present model is intended for illustrative purposes only, and not as a proposed prediction for wind wave development. A more realistic model should at least account for the depletion of energy from the shear layer as well as various wave dissipation mechanisms.

As a further illustration of the naure and affect of the instability mechanism, results of an integration showing the amplification factor $A(\lambda)$ of a Fourier coefficient and the time $T(\lambda)$ to restabilization are shown in figure 5 for the case $u/c_m = 2.0$. $T(\lambda)$ is the time at which the mode of wavelength λ stabilises according to the assumed linear increase of the drift layer thickness, and A is given by

$$A(\lambda) = \exp\left(\int_0^T \sigma(\lambda, t)\, dt \right). \tag{3.2}$$

8

The amplification factor is very sensitive to the rate of growth of the drift layer. According to the numerical results,

$$\log A_{\max} \sim 2.8 \, 10^{-2} u \sigma^+ \lambda_m / (\kappa c_m^2), \quad T_{\max} = 0.54 \lambda_m / (\kappa u), \tag{3.3}$$

where $_{\max}$ refers to the wavelength which is amplified most by the process. This wavelength is found numerically to be close to λ_m.

4. Discussion

The presence of this instability appears to have been first noticed by Valenzuela (1976) who performed a numerical study of the Orr-Sommerfeld equation for a coupled shear flow. He concluded: "When shear flow in the water is included a significant increase in the growth rates is obtained, in particular for wind speeds in excess of 6 m/s." We consider that the main contribution of our present work is to expose the inviscid, hydrodynamic structure of this instability, and to provide relatively simple and explicit formulae to permit the study of its dependence on various parameters which may alter the wind drift layer.

Experimental support of this mechanism can be found in the report of Huang, Bliven and Long (1988) on laboratory study of generation of waves by wind from a flat calm. They found that when the wind speed is higher than a threshold value of around 6 m/sec, the growth of waves becomes spontaneous (see their figures 3.6 and 3.10). They also proposed that the phenomena must be due to an instability mechanism, and the Kelvin-Helmhotz instability was suggested as a possible candidate, but a detailed comparison was not made. The critical air speed for the Kelvin-Helmholtz instability is $U_{KH} = \sqrt{\rho/\rho_a}c_m \doteq$ 6.4 m/sec. The phase speed of the Kelvin-Helmholtz unstable waves is $\rho_a U/\rho$. When applied to the case of generation of waves by wind, the minimum wind speeds required and phase speeds of the unstable waves for the present mechanism and the Kelvin-Helmholtz instability are comparable, but the two mechanisms are fundamentally different. First, the Kelvin-Helmholtz instability predicts the growth rate to increase with wavenumber, unlike the present one which is highly selective in wavelength and actually predicts a wavelength of maximum instability for a given drift speed and drift layer thickness. Second, the present mechanism predicts a shifting towards longer waves with time (frequency downshifting) due to the thickening of the wind drift layer to which the Kelvin-Helmholtz mechanism is not sensitive. Third, the present mechanism does not rely on air density or motion, and applies equally to situations where the drift is generated by other means. Finally, our analysis also yields stable propagating waves in the presence of the instability which are absent in the Kelvin-Helmholtz analysis. Yet we do not see any reason why these two

mechanisms cannot coexist.

The fact that the present mechanism responds to the drift current rather than to the air-water shear flow gives it additional implications. For example, if the near surface current structure, associated with longer waves, shear flows or internal waves, is such that it selectively enhances or reduces the vorticity and/or the drift layer thickness, then it will be reflected by the differential growth of the waves under this mechanism. This has particular relevance to ocean remote sensing by high-frequency synthetic aperture radar which relies on a rapid response of short waves to current structure. The simplicity of the present approach allows related mechanism, such as the effects of surfactants and the destruction of short wind waves by long waves, to be examined by simple models.

Acknowledgement

References

Baum, E. 1977 Characterization of the wind-driven surface drift current. A theoretical description. TRW Rep 31326-6010-RU-OO.

Huang, N.E., Bliven, L.F. & Long, S.R. 1988 On the properties of the water surface roughness structure under the action of wind and waves. Submitted, J. Fluid Mech.

MacKay, R.S. & Saffman, P.G. 1986 Stability of water waves. Proc. Roy. Soc. A 406, 115-125.

Miles, J.W. 1957 On the generation of surface waves by shear flows. J. Fluid Mech. 3, 185-204.

Milinazzo, F.A. & Saffman, P.G. 1989 Effect of a thin wind drift layer on capillary-gravity waves of permanent form.

Phillips, O.M. 1957 On the generation of waves by turbulent wind. J. Fluid Mech. 2, 417-445.

Valenzuela, G.R. 1976 the growth of gravity-capillary waves in a coupled shear flow. J. Fluid Mech. 76, 229-250.

Voronovich, A.G., Lobanov, E.D. & Rybak, S.A. 1980 On the stability of gravitational-capillary waves in the presence of a vertically nonuniform current. Izv. Atm. and Ocean Phys. 16, 220-222.

Figure captions

Figure 1. The wedge of instability in the $q - \beta$ plane.

Figure 2. Range of unstable wavelengths and contours of constant growth rate *vs* drift layer thickness for varying drift velocity. (*a*) $u/c_m = 1.25$. (*b*) $u/c_m = 1.5$. (*c*) $u/c_m = 1.75$. (*d*) $u/c_m = 2.0$. + denotes the location of the maximum growth rate. Interior contour gives locus of the growth rate of one-half the maximum.

Figure 3. Dependence of critical $_{crit}$ and maximum $^+$ growth rate values on u/c_m. (*a*) Wavelength behaviour. (*b*) Drift layer depth. (*c*) Maximum growth rate and phase speeds.

Figure 4. Development of a wavenumber spectrum from background noise for $u/c_m = 2$. Power is plotted against wavenumber at intervals of 0.2 sec.

Figure 5. Amplification factor and growth lifetime of Fourier coefficients for a linearly growing drift layer *vs* wavelength for $u/c_m = 2$. Scales are given by equation (3.3).
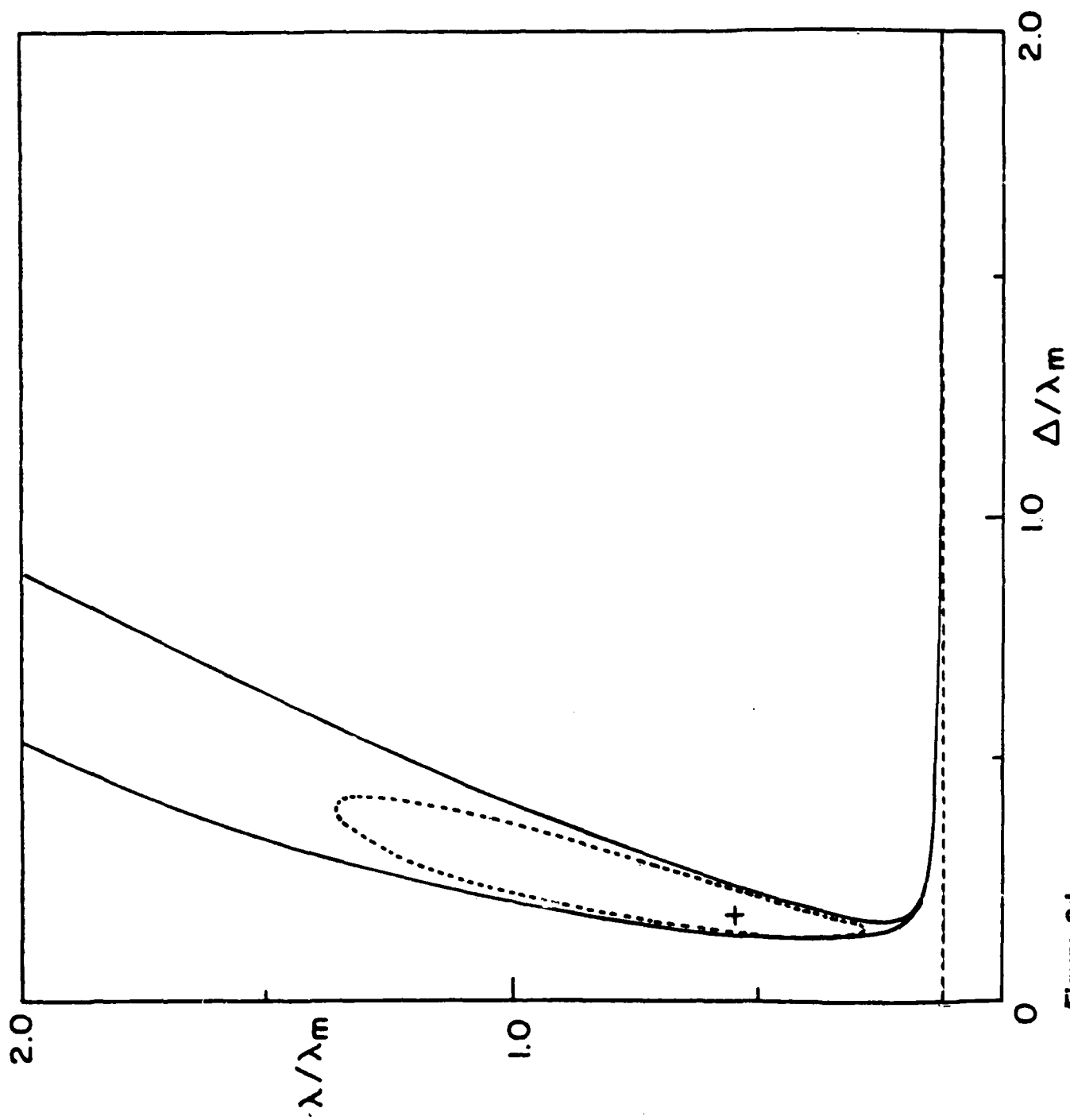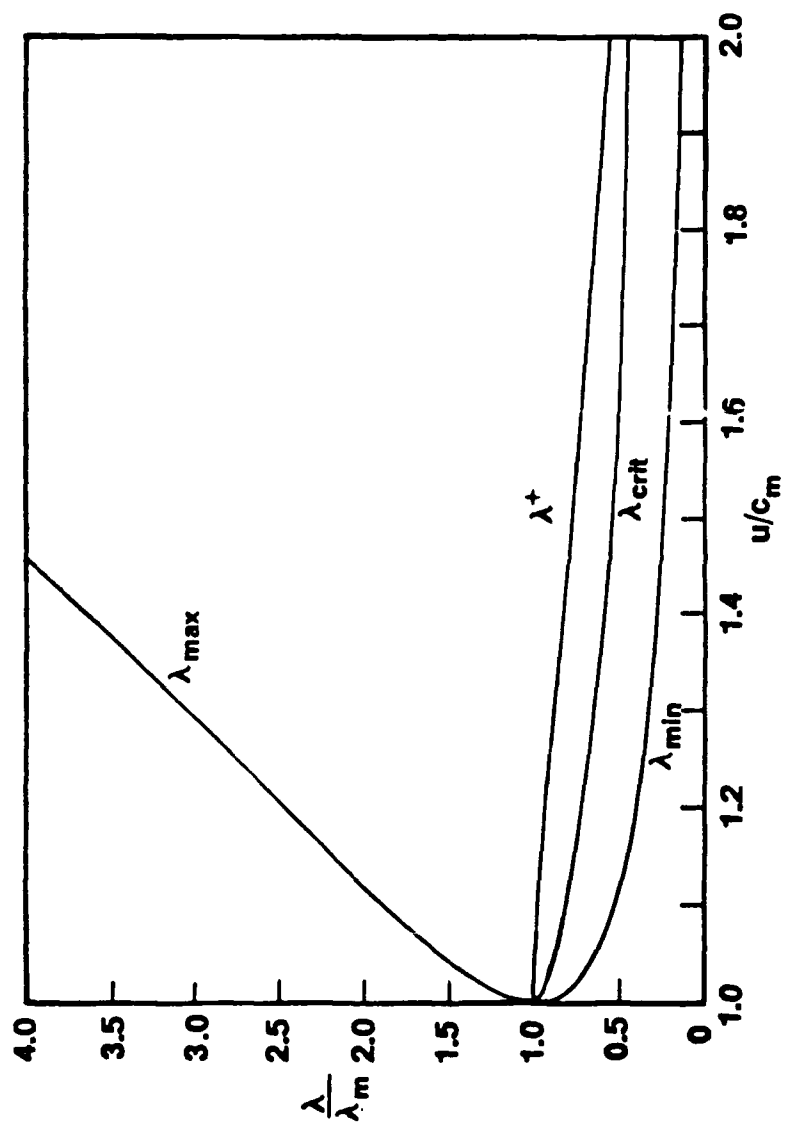
UNSTABLE

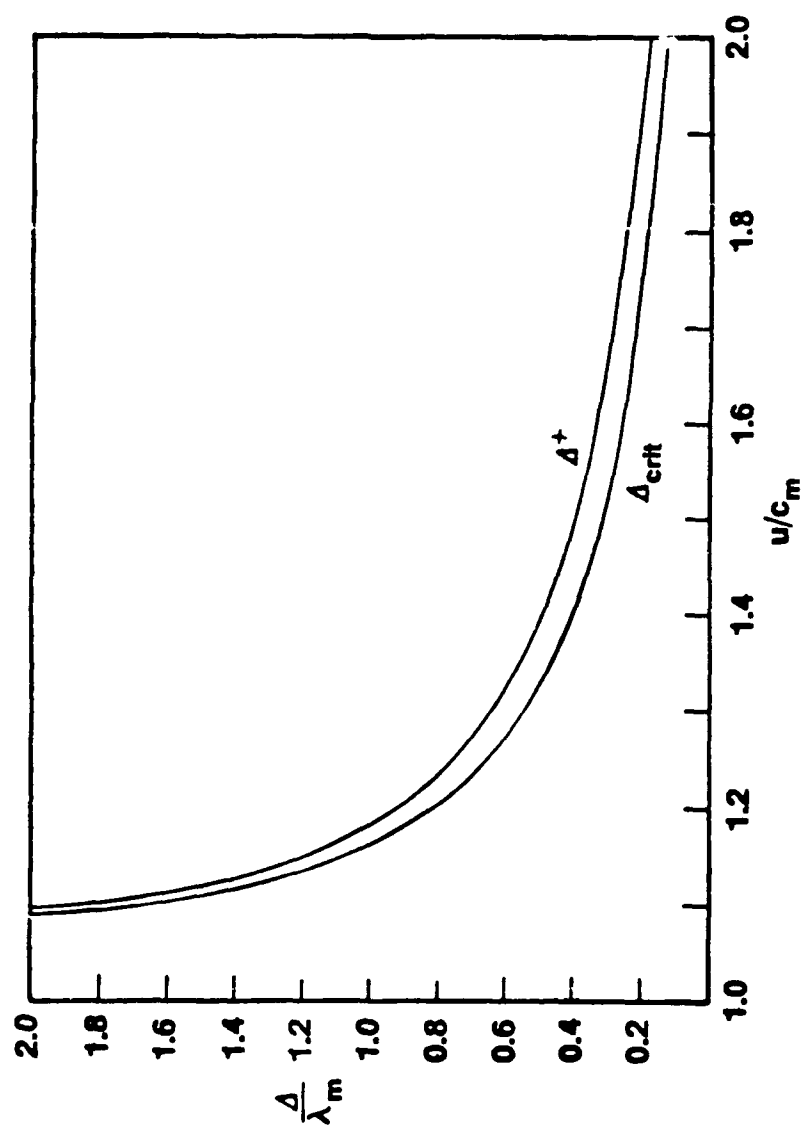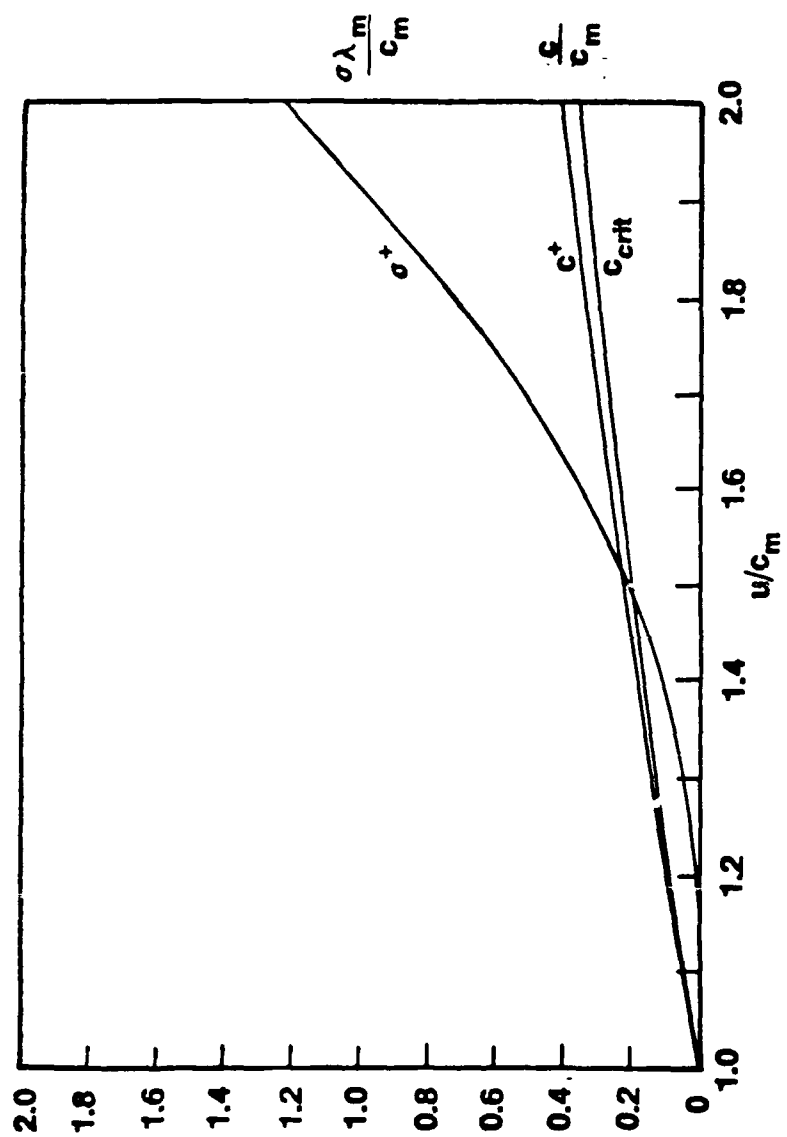β

q
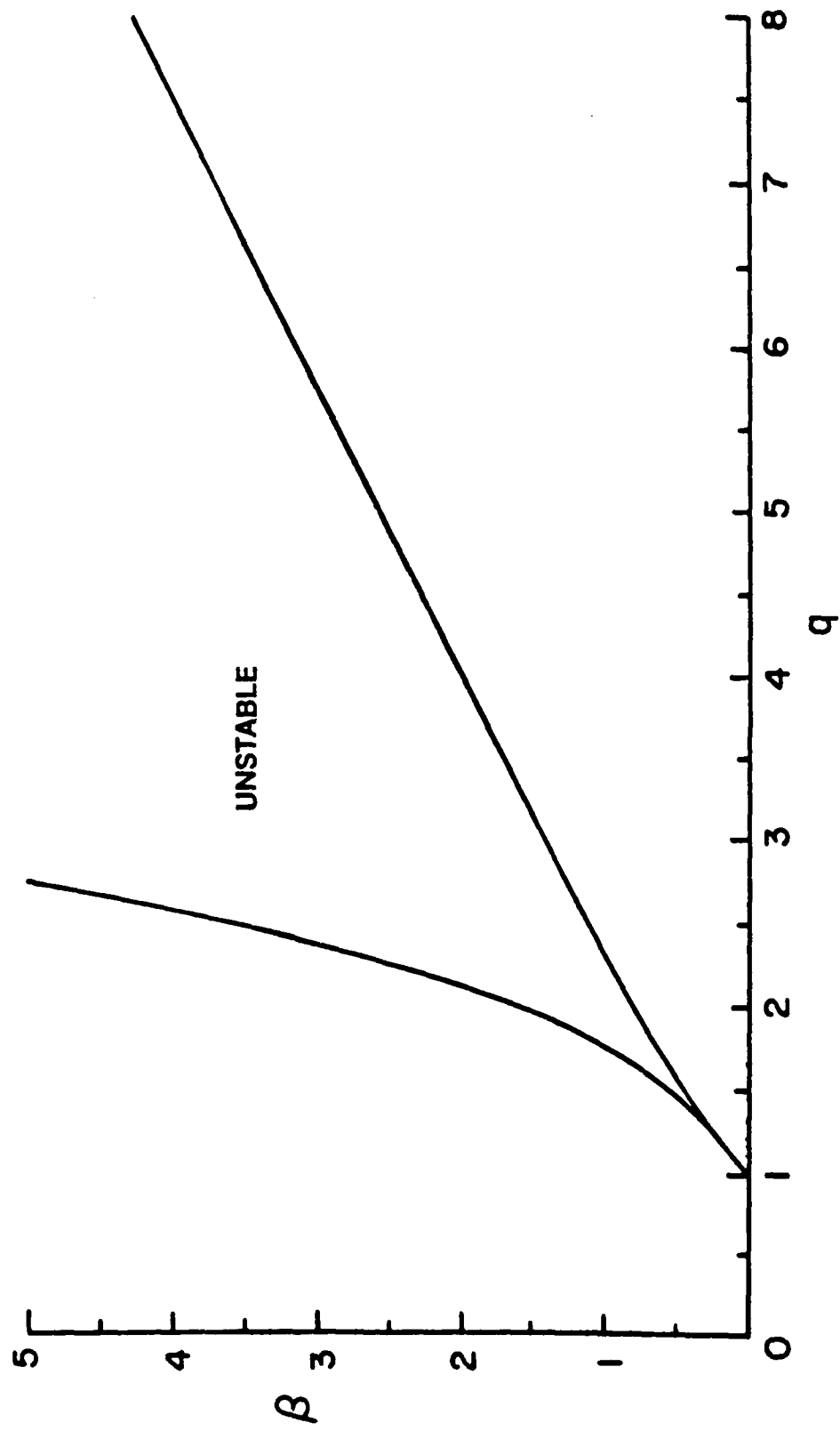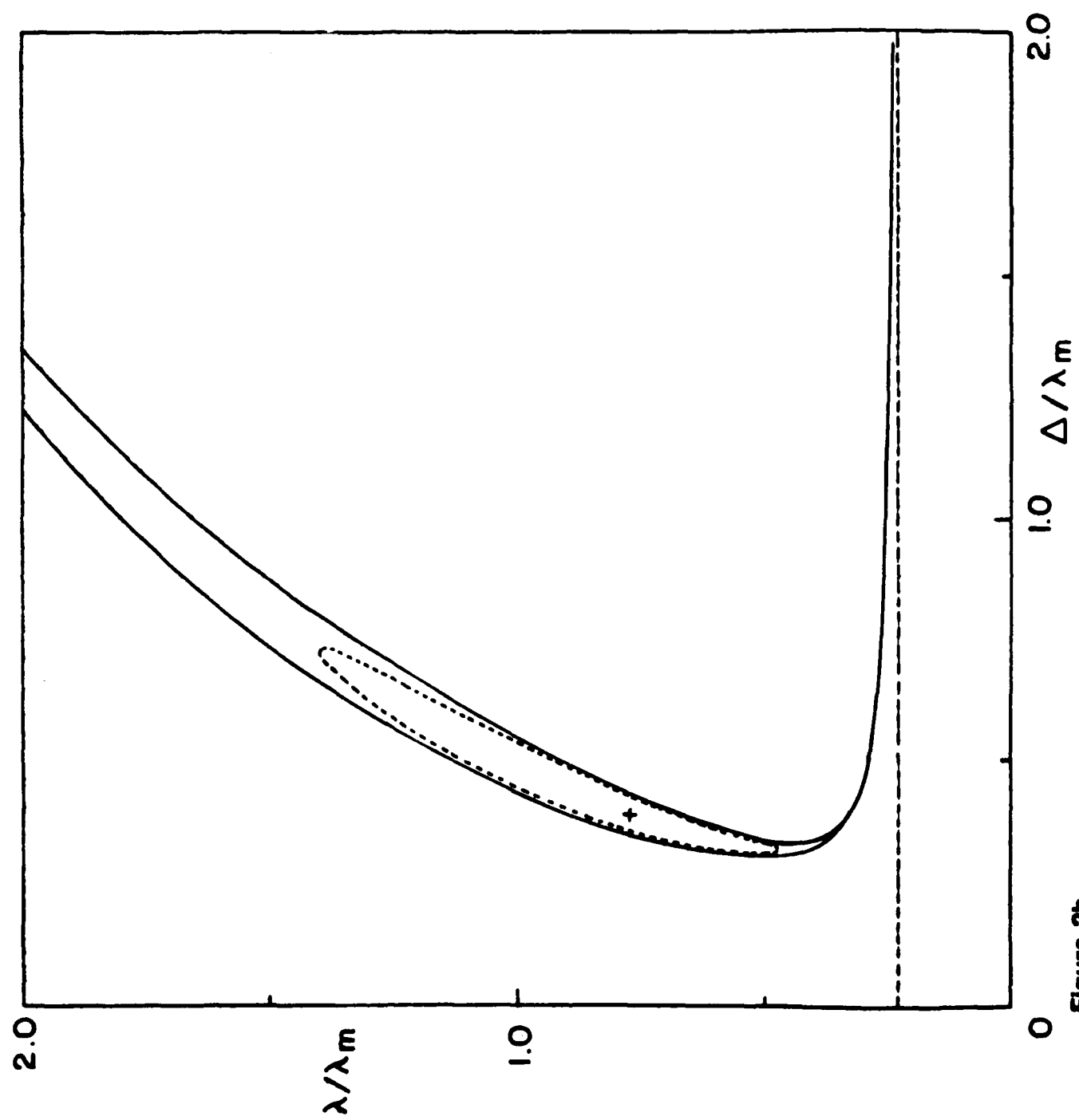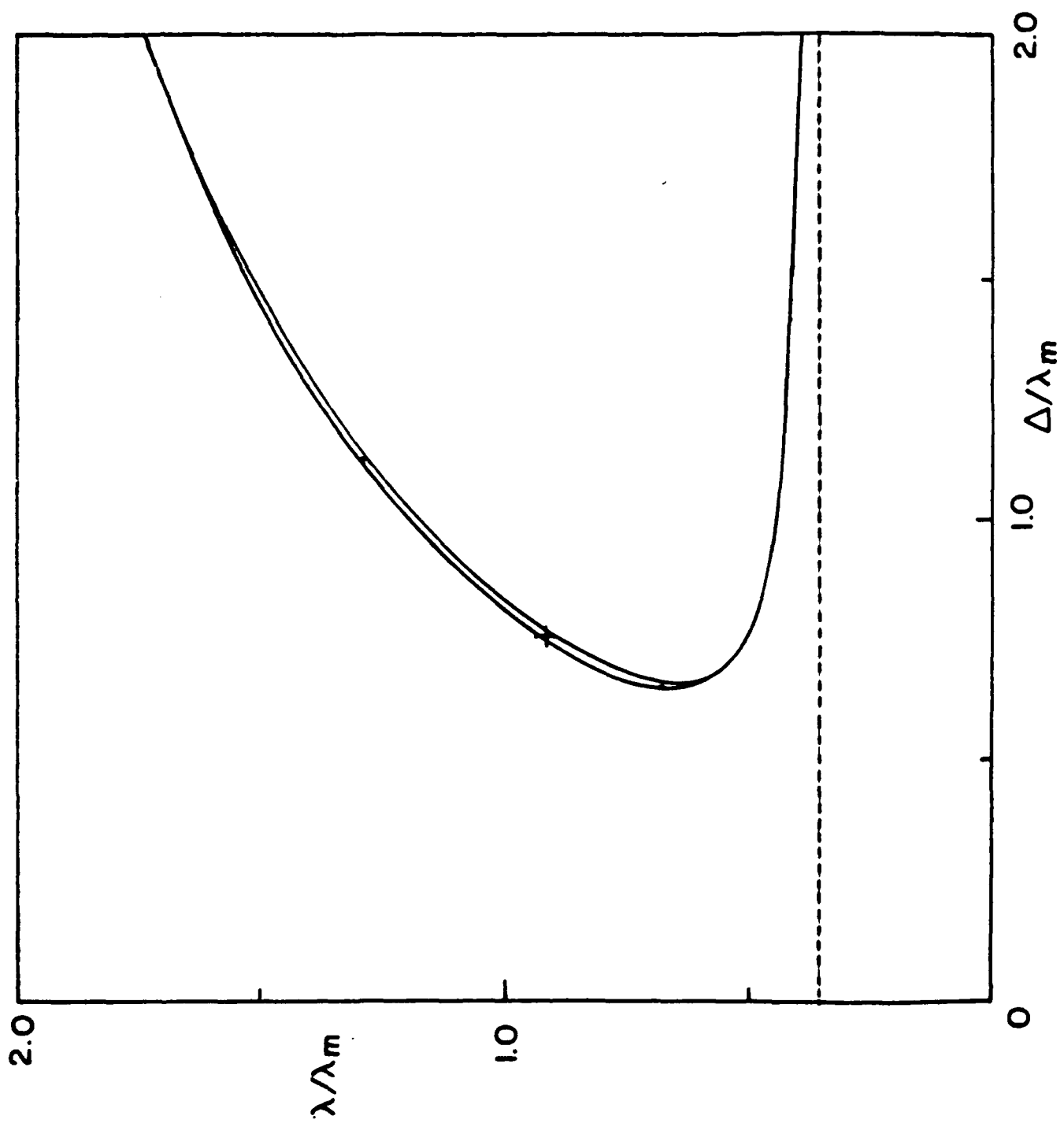
Figure 1

Figure 2b

Figure 2a
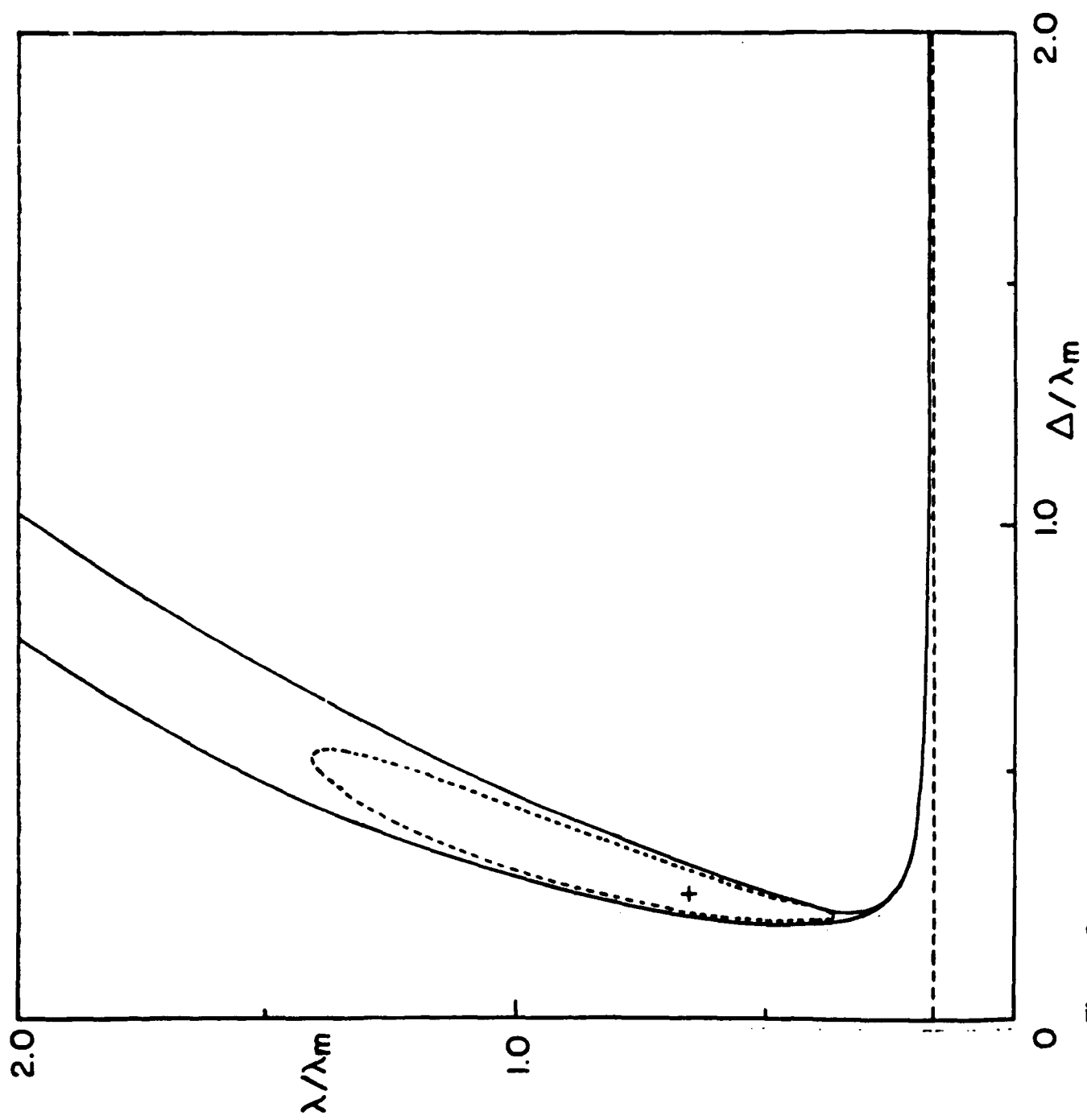
Figure 2c

Figure 2d

Figure 3a

Figure 3b

Figure 3c

Figure 4

Figure 5